

One-step synthesis of ternary nanostructured CuO/Ti_{0.8}Ce_{0.2}O₂ catalysts for low temperature CO oxidation

Jing Huang · Yanfei Kang · Taili Yang · Yao Wang · Shurong Wang

Received: 17 February 2011 / Accepted: 7 June 2011 / Published online: 17 June 2011
© Akadémiai Kiadó, Budapest, Hungary 2011

Abstract Ternary nanostructured CuO/Ti_{0.8}Ce_{0.2}O₂ catalysts were prepared by a one-step surfactant-assisted method of nanoparticle assembly. The textural and structural properties of the CuO/Ti_{0.8}Ce_{0.2}O₂ catalysts were characterized by XRD, TGA, BET, XPS and H₂-TPR. Their catalytic performance for low-temperature CO oxidation was studied by using a catlab system. CuO supported on binary Ti_{0.8}Ce_{0.2}O₂ support showed higher catalytic activity than CuO supported on single CeO₂ or TiO₂ support. The calcination temperature had a remarkable influence on the catalytic activity of the CuO/Ti_{0.8}Ce_{0.2}O₂ catalysts. The CuO/Ti_{0.8}Ce_{0.2}O₂ catalyst calcined at 500 °C exhibited the highest catalytic activity with T_{50%} and T_{100%} at 82 and 123 °C, respectively. According to the XRD, BET and H₂-TPR analyses, the higher surface areas and more highly dispersed small particle size CuO should be responsible for the high catalytic activity of catalysts.

Keywords CuO/Ti_{0.8}Ce_{0.2}O₂ catalysts · Low temperature · CO oxidation · One-step synthesis

Introduction

CO as a major toxic air pollutant, which is usually emitted by products of combustion processes from industrial, transportation and domestic activities, is always the central issue in the environmental protection field. A number of studies have demonstrated that supported noble metal (such as Au and Pt) catalysts have high catalytic activities for low-temperature CO oxidation [1, 2]. However, due to

J. Huang
Sinopec Research Institute of Petroleum Engineering, Beijing 100101, China

Y. Kang · T. Yang · Y. Wang · S. Wang (✉)
Department of Chemistry, Nankai University, Tianjin 300071, China
e-mail: shrwang@nankai.edu.cn

high prices and the scarcity of noble metals, attention has been given to search an alternative catalytic component to reduce using or even replace the noble metals. Transition metals supported on some metal oxides are good substitute catalysts because of their low price and widespread use. Among them, copper-based catalysts attract special interest due to their low price and greater activity compared to other transition metals like Co, Ni, Cr, and Zn [3, 4]. Recent research has demonstrated that highly dispersed CuO on reducible metal oxides such as TiO₂ [5], α -Fe₂O₃ [6] and CeO₂ [7–10] has high activity for CO oxidation.

It is well known that CeO₂ increases the dispersion of active components and its most important property is to serve as an oxygen reservoir which stores and releases oxygen via the redox shift between Ce⁴⁺ and Ce³⁺ under oxidizing and reducing conditions [9, 10]. Furthermore, in order to increase the thermal stability and redox property of the CeO₂ support, some mixed oxides are prepared by adding anti sintered oxides like TiO₂ [11, 12]. Zhu et al. [11] have studied Pd supported on CeO₂–TiO₂ mixed oxide catalyst for CO oxidation and found that the special Pd–Ce–Ti interaction was favorable to the reduction of PdO and interfacial CeO₂ species. Lamalle and co-workers [12] prepared the Au/Ce_{0.3}Ti_{0.7}O₂ catalysts via deposition, precipitation and impregnation methods, and found that the preparation method or the choice of the precipitating agent has an important effect on the activity of the gold-based catalyst.

In binary CuO/CeO₂ catalysts, a strong catalytic synergy between CuO and CeO₂ has ever been found [7–10]. However, as far as we know, little attention has been paid to the ternary CuO/Ti_xCe_{1-x}O₂ catalysts for low-temperature CO oxidation. The supported catalysts are usually prepared by the two-step method [13, 14]. First, the support is prepared by the sol–gel method or the co-precipitation method. Second, the active component such as Au or CuO is supported on the support by the impregnation method. However, after conventional impregnation, the surface area decreases dramatically, probably due to partial porous blocking and enhanced support crystallization.

Herein, the CuO/Ti_{0.8}Ce_{0.2}O₂ catalysts are prepared by a simple, one-step surfactant-assisted method of nanoparticle assembly. The textural and structural properties of CuO/Ti_{0.8}Ce_{0.2}O₂ catalysts are characterized by XRD, TGA, BET, XPS and H₂-TPR. The effect of the calcination temperature on the catalytic activity of CuO/Ti_{0.8}Ce_{0.2}O₂ is investigated. For comparison, the catalytic performance of CuO/TiO₂ and CuO/CeO₂ prepared by the same method is also studied.

Experimental

Catalyst preparation

20 mol % CuO/Ti_{0.8}Ce_{0.2}O₂ catalysts were synthesized using a one-step surfactant-assisted method of nanoparticle assembly. At room temperature, 6 mmol cetyltrimethylammonium bromide (CTAB) was dissolved in 200 mL distilled water under ultrasound irradiation for 15 min, then 20 mmol Cu(NO₃)₂·3H₂O and the appropriate amount of Ti(SO₄)₂ and Ce(NO₃)₄·6H₂O were added under vigorous stirring.

After 0.5 h, 0.2 mol/L NaOH was added gradually until the pH of the mixture was 10. After further stirring for 12 h, the suspension was aged at 90 °C for 3 h, washed with hot water, dried at 80 °C for 8 h, then milled and calcined at different temperatures (400, 500, 600, 700 and 800 °C, respectively) for 4 h in air. For comparison, CuO/TiO₂ and CuO/CeO₂ were also prepared by the same method and calcined at 500 °C.

Catalyst characterization

Thermogravimetric analysis (TGA, Mettler 851e) was performed with a heating rate of 10 °C/min in a static air atmosphere, using α -Al₂O₃ as the reference. X-ray diffraction (XRD) patterns were measured on a Philips XPERT MPD X-ray diffractometer with Cu K α radiation ($\lambda = 1.5418 \text{ \AA}$) in a 2θ range of 20–80°. The specific surface areas were calculated following multi-point Brunauer–Emmett–Teller (BET) procedure on a Micromeritics TriStar 3000 instrument at liquid N₂ temperature. Temperature-programmed reduction (TPR) experiments were performed in a mixture of flowing 5% H₂ in Ar (30 mL/min) over 50 mg catalyst with a heating rate of 10 °C/min. X-ray photoelectron spectra (XPS) were obtained on a Kratos Axis Ultra Spectrometer with a monochromatic AlK α source ($E = 1486 \text{ eV}$). FT-IR spectra were recorded on a Shimadzu IRPrestige-21 spectrometer in absorbance mode, by averaging 250 scans at 0.5 cm⁻¹ resolution.

Catalytic activity

Temperature-programmed (light-off) reactions were carried out in a Hiden catlab system. 50 mg catalyst was loaded into the quartz micro-reactor. The gas product composition was analyzed using a Hiden quadrupole mass spectrometer (HPR20). CO oxidation was studied under steady-state conditions, using a certified gas mixture containing 1000 ppm CO and 10% O₂ in N₂(Praxair), at a constant flow rate of 50 cm³/min.

Results and discussion

TGA was performed to study the thermal decomposition behavior of the as-synthesized materials. Fig. 1 depicts the TG curve of the CuO/Ti_{0.8}Ce_{0.2}O₂ catalyst dried at 80 °C. It is clear that the weight loss is continuous starting at room temperature and up to approximately 500 °C. Three sharp weight losses are observed. The first weight loss from room temperature to 175 °C may be attributed to desorption of non-dissociatively adsorbed water as well as water held on the surface by hydrogen bonding. The second weight loss from 175 to 240 °C may be due to the loss of water held in the pores and partial de-hydroxylation of the surface. The third loss from 240 to 500 °C may result from the decomposition of the surfactant and the combustion of carbon species. After 500 °C, the weight of the precursor no longer changes, which indicates that the carbon species (surfactant molecules) in the sample can be completely removed after calcination at 500 °C in air.

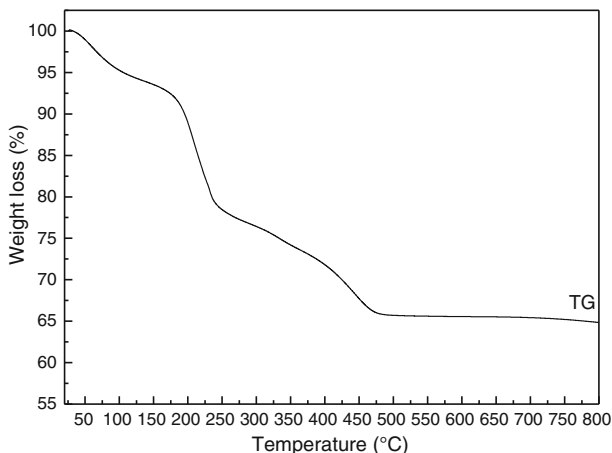


Fig. 1 TG curve of $\text{CuO}/\text{Ti}_{0.8}\text{Ce}_{0.2}\text{O}_2$ dried at 80 °C

Fig. 2 presents the XRD patterns of the prepared $\text{CuO}/\text{Ti}_{0.8}\text{Ce}_{0.2}\text{O}_2$ catalysts calcined in the temperature range from 400 to 800 °C, together with the CuO/TiO_2 and CuO/CeO_2 catalysts calcined at 500 °C.

In order to avoid any misconception of the phases formed in the mixed oxide catalysts, XRD pattern of pure CuO has also been included in Fig. 2. The crystal phase of TiO_2 in CuO/TiO_2 (Fig. 2a) contains both anatase and rutile. Moreover, the CuO diffraction peaks at $2\theta = 35.5$ and 38.6° can be observed clearly, indicating larger particle size of bulk CuO . The reflections in the CuO/CeO_2 sample well correspond to the cubic, fluorite structure of CeO_2 . The lack of CuO peaks suggests that CuO particles are amorphic, too small to be detected by XRD. The two $\text{CuO}/$

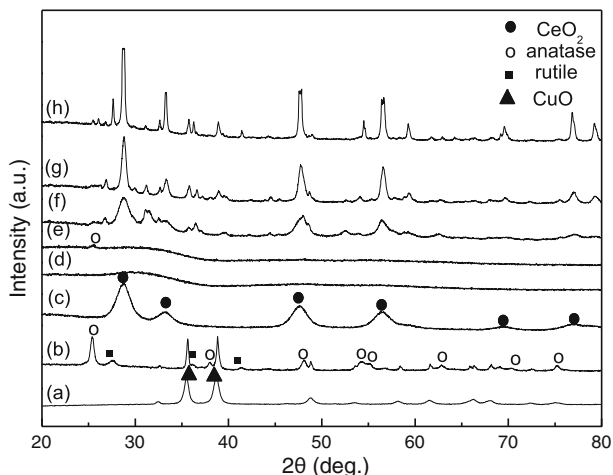


Fig. 2 XRD patterns of CuO (a), CuO/TiO_2 (b), CuO/CeO_2 (c) and $\text{CuO}/\text{Ti}_{0.8}\text{Ce}_{0.2}\text{O}_2$ calcined at 400 (d), 500 (e), 600 (f), 700 (g), and 800 °C (h)

Ti_{0.8}Ce_{0.2}O₂ samples calcined at 400 and 500 °C exhibit very broad peaks due to amorphous state, with only a little of anatase phase in the sample calcined at 500 °C. According to the literature data [13, 15], this result means that the addition of a small amount of CeO₂ into TiO₂ inhibits the transition phase of TiO₂ from anatase to rutile. On the other hand, no distinct characteristic reflections of the CuO structure are present in the two samples, which may be due to high dispersion of CuO nanoparticles with too small particle sizes to be identified by the conventional XRD method. When the sample was calcined at 600 °C, the cubic phase of CeO₂, both anatase and rutile phase of TiO₂ can be clearly observed. Meanwhile, the CuO diffraction peaks at $2\theta = 35.5$ and 38.6° can also be observed clearly. As the calcination temperature further increases, the CeO₂, TiO₂ and CuO crystalline peaks all become sharper and sharper, indicating their particle sizes become larger and larger. The average sizes of CuO particles (D_{CuO}) were calculated by using the Scherrer equation with the half width of the CuO reflection peak at 35.5°. The D_{CuO} in the CuO/Ti_{0.8}Ce_{0.2}O₂ catalysts calcined at 600, 700 and 800 °C is 22.6, 32.4 and 45.2 nm, respectively.

The above XRD results are in good accordance with the information of specific surface areas obtained for the CuO/Ti_{0.8}Ce_{0.2}O₂ samples calcined at different temperature (Table 1). By comparing the surface areas of the samples calcined at different temperatures, it can be seen that the surface area decreases with the increase of the calcination temperature. The CuO/Ti_{0.8}Ce_{0.2}O₂ calcined at 400 °C shows the largest surface area of 180 m²/g. However, the surface area sharply declines to 70 m²/g when the calcination temperature increases to 600 °C, and drops to only 2 m²/g at the calcination temperature of 800 °C. The results indicate that the calcination temperature also plays an important role in affecting the surface areas of the catalysts.

Fig. 3 shows typical H₂-TPR profiles of CuO/TiO₂, CuO/CeO₂ and CuO/Ti_{0.8}Ce_{0.2}O₂ calcined at 500 °C. When the temperature was below 400 °C, the TPR profile of CuO/TiO₂ shows mainly two reduction peaks at about 204 and 228 °C. Similarly, the TPR profile of CuO/CeO₂ shows two reduction peaks at about 169 and 190 °C. The TPR profile of CuO/Ti_{0.8}Ce_{0.2}O₂ shows two overlapping peaks at about 175 and 186 °C. Compared to the pure CuO, which shows a single peak of maximum hydrogen consumption at about 373 °C [16], the reduction peaks of

Table 1 Average sizes of CuO particles (D_{CuO}), surface area, $T_{50\%}$ and $T_{100\%}$ of CuO/Ti_{0.8}Ce_{0.2}O₂ catalysts calcined at different temperatures

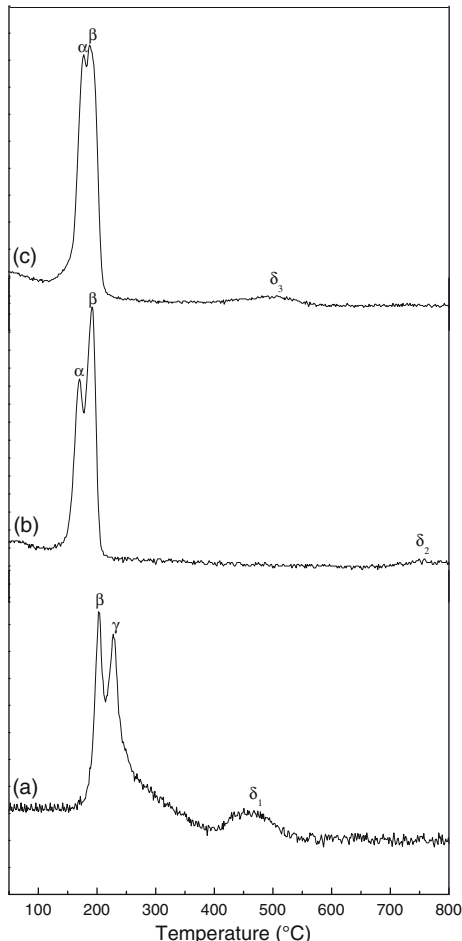
Catalysts	D_{CuO} (nm)	S_{BET} (m ² g ⁻¹)	$T_{50\%}$ (°C)	$T_{100\%}$ (°C)
CuO/TiO ₂ (500)	30.1	91	163	300
CuO/CeO ₂ (500)	–	105	102	144
CuO/Ti _{0.8} Ce _{0.2} O ₂ (400)	–	180	92	180
CuO/Ti _{0.8} Ce _{0.2} O ₂ (500)	–	145	82	123
CuO/Ti _{0.8} Ce _{0.2} O ₂ (600)	22.6	70	139	243
CuO/Ti _{0.8} Ce _{0.2} O ₂ (700)	32.4	21	175	274
CuO/Ti _{0.8} Ce _{0.2} O ₂ (800)	45.2	2	193	317

copper species in our case are much lower. This may be due to the synergistic effects between CuO and the supports which were promoting the reduction of CuO. Meanwhile, the reduction peaks of copper species in CuO/CeO₂ and CuO/Ti_{0.8}Ce_{0.2}O₂ are lower than that of CuO/TiO₂. According to the literature [17–19], the lower temperature α peaks at 169 and 175 °C are ascribed to the reduction of highly dispersed CuO interacting strongly with the support, which are regarded as the active sites for CO oxidation, the higher temperature β peaks at 186, 190 and 204 °C are assigned to the reduction of larger CuO particles less associated with the support, and the high temperature γ peak at 228 °C in the CuO/TiO₂ sample is ascribed to the reduction of bulk CuO which associated with TiO₂ to some extent. The higher reduction peaks (δ_1 , δ_2 and δ_3) result from the reduction of the supports. The δ_1 reduction peak centered at 460 °C in the CuO/TiO₂ sample may be due to the reduction of oxygen on the TiO₂ surface and the reduction of TiO₂ interacting with CuO [20]. The weak δ_2 reduction peak centered at 750 °C in the CuO/CeO₂ sample may be assigned to the reduction of bulk-phase lattice oxygen in the CeO₂ support [21, 22]. The δ_3 reduction peak centered at 500 °C in the CuO/Ti_{0.8}Ce_{0.2}O₂ sample may be attributed to the reduction of the surface capping oxygen ions on the Ti_{0.8}Ce_{0.2}O₂ support and the reduction of the support interacting with CuO [12, 20].

XPS was performed to illuminate the surface composition of the studied metal oxides and to acquire detailed information on the chemical states of the cations and anions. XPS analysis reveals the presence of Cu, Ti, Ce and O on the surface of the CuO/Ti_{0.8}Ce_{0.2}O₂ catalyst calcined at 500 °C. The surface composition of the CuO/Ti_{0.8}Ce_{0.2}O₂ catalyst is estimated by XPS. The surface atomic contents of Cu, Ti and Ce are 7.20, 22.66 and 5.71%, in order. The surface atomic ratio of Cu/(Cu + Ti + Ce) is 0.202, which is approximately consistent with the nominal atomic ratio (0.20). The spectra of Ce3d, Ti2p and Cu2p binding energies are presented in Fig. 4. In Fig. 4a, the Ce3d spectrum shows five peaks at about 881.9, 888.9, 897.8, 900.5 and 907.7 eV. The principal peaks of Ce3d_{3/2} and Ce3d_{5/2} are centered at about 900.5 and 881.9 eV, respectively. The difference between the principal binding energies for Ce3d_{3/2} and Ce3d_{5/2} is in agreement with the expected value of 18.6 eV, indicating the main valence of Ce atom was +4 [23, 24]. Two weak peaks at about 883.0 and 903.7 eV are the characteristic peak of Ce₂O₃, proving the existence of the Ce⁴⁺/Ce³⁺ re-dox couple in the CuO/Ti_{0.8}Ce_{0.2}O₂ catalyst. The weak characteristic peaks of Ce₂O₃ in XPS spectra and no crystallite peaks due to Ce₂O₃ in XRD pattern indicate the low Ce₂O₃ content in the CuO/Ti_{0.8}Ce_{0.2}O₂ catalyst.

The peaks of Ti2p_{1/2} and Ti2p_{3/2} are centered at about 463.9 and 458.2 eV, respectively (Fig. 4b). The binding energy difference between the Ti2p_{1/2} and Ti2p_{3/2} photoemission feature is 5.7 eV. This value is in excellent agreement with the reported value of Ti⁴⁺ [25]. In Fig. 4c, the peaks centered at about 932.5 and 952.5 eV represent the Cu2p_{3/2} and Cu2p_{1/2}, respectively. Avgouropoulos and Ioannides [26] reported that the presence of shake-up peaks (about 939–944 eV) and a higher Cu2p_{3/2} binding energy (about 933.0–933.8 eV) are two major XPS characteristics of CuO, while a lower Cu2p_{3/2} binding energy (about 932–933 eV) and the absence of the shake-up peak are the characteristics of reduced copper species. In the case of the catalyst spectra, the Cu2p_{3/2} spectra contain a shake-up

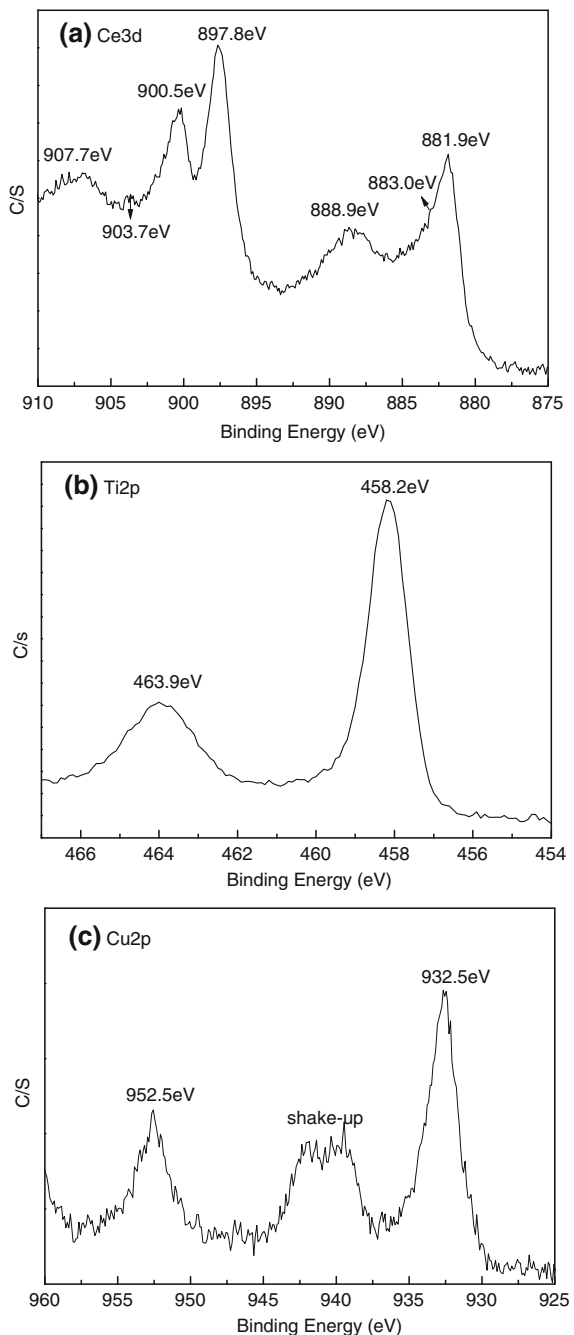
Fig. 3 H₂-TPR profiles of CuO/TiO₂ (a), CuO/CeO₂ (b) and CuO/Ti_{0.8}Ce_{0.2}O₂ (c) calcined at 500 °C



peak at 938–944 eV, which indicates Cu²⁺ species exist in the catalyst. Meanwhile, the lower Cu2p_{3/2} binding energy suggests the presence of reduced copper species in the catalyst. However, it is less convincing to distinguish between Cu₂O and Cu⁰ because the Cu2p_{3/2} binding energies and peak shapes of Cu₂O and Cu⁰ are essentially identical [27]. The formation of the reduced copper species may result from strong interaction of copper oxide with the support [28] or may occur under the procedure of XPS measurement [29].

Fig. 5 shows the FT-IR spectrum of CO adsorbed on the CuO/Ti_{0.8}Ce_{0.2}O₂ catalyst (calcined at 500 °C) at room temperature. One strong band with good symmetry can be clearly observed at 2123.3 cm⁻¹. It is well-known that the bands in the 2110–2143 cm⁻¹ region are assigned to Cu⁺-CO surface complexes, while the band at 2097 cm⁻¹ is assigned to Cu⁰-CO. Meanwhile, Cu²⁺-CO species are reported to be unstable at room temperature, and are observed only at low temperatures or at high CO pressures [30]. Accordingly, the band at 2123.3 cm⁻¹ is

Fig. 4 XPS of CuO/Ti_{0.8}Ce_{0.2}O₂ catalyst calcined at 500 °C: Ce3d (**a**), Ti2p (**b**) and Cu2p (**c**)



assigned to the stretching mode of CO adsorbed on Cu⁺, indicating the existence of Cu⁺. Therefore, combining the result of XPS, it is suggested that both Cu²⁺ and Cu⁺ species coexist in CuO/Ti_{0.8}Ce_{0.2}O₂ catalyst.

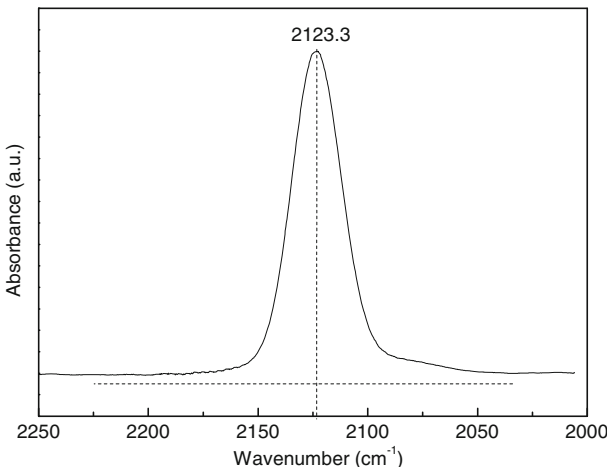


Fig. 5 FT-IR spectrum of CO adsorbed on the CuO/Ti_{0.8}Ce_{0.2}O₂ catalyst

The light-off curves of the CuO/Ti_{0.8}Ce_{0.2}O₂ catalysts calcined at different temperatures are presented in Fig. 6. It can be observed that CO conversion increases with the increase of reaction temperature for all the prepared catalysts. The temperature of 50 and 100% CO conversion ($T_{50\%}$ and $T_{100\%}$) of the CuO/Ti_{0.8}Ce_{0.2}O₂ catalysts are listed in Table 1. The catalytic activity of the CuO/Ti_{0.8}Ce_{0.2}O₂ catalysts increases with the increase of calcination temperature from 400 to 500 °C, but decreases from 500 to 800 °C. The catalyst calcined at 500 °C with higher surface area and smaller particle size exhibits the highest catalytic activity on CO oxidation with $T_{50\%}$ and $T_{100\%}$ at 82 and 123 °C, respectively. The catalyst calcined at 800 °C, having the lowest surface area of 2 m²/g and the largest particle size, shows the lowest activity with $T_{50\%}$ at 193 °C. The XRD and BET analyses have revealed that the increase of calcination temperature made the decrease of the surface areas and the increase of particle sizes. Thus, the observed difference in the catalytic activities the CuO/Ti_{0.8}Ce_{0.2}O₂ catalysts calcined at different temperatures maybe due to the agglomeration of the catalysts, the decrease of the surface areas, and the increase of the particle size with increasing the calcination temperature. Specially, the catalyst calcined at 400 °C with the largest surface area of 180 m²/g has high activity with $T_{50\%}$ at 92 °C, however, which is lower activity than the catalyst calcined at 500 °C. This can be explained well by the TGA results. The carbon species (surfactant molecules) in the samples could be completely removed after calcination at 500 °C in air. The large surface area can provide a large surface to volume ratio, which is believed to enhance the catalytic activity, but the remained carbon species in the catalyst calcined at 400 °C has a negative effect on the improved catalytic activity.

For comparison purposes, the catalytic activities of the CuO/TiO₂ and CuO/CeO₂ catalysts calcined at 500 °C are included in Fig. 7, together with the CuO/Ti_{0.8}Ce_{0.2}O₂ catalysts calcined at 500 °C. CuO supported on binary Ti_{0.8}Ce_{0.2}O₂ support shows higher catalytic activity than CuO supported on single CeO₂ or TiO₂.

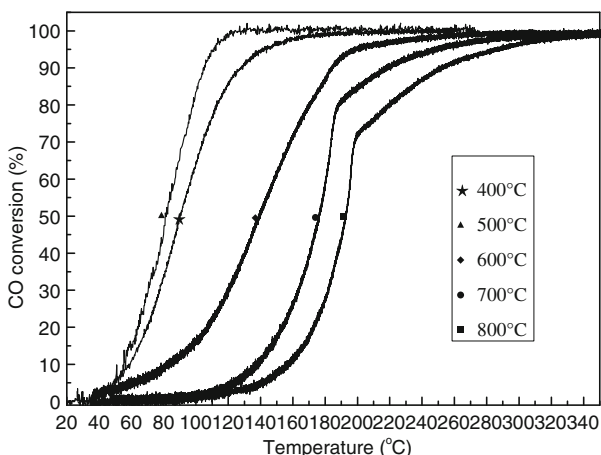


Fig. 6 Catalytic activity for CO oxidation of $\text{CuO}/\text{Ti}_{0.8}\text{Ce}_{0.2}\text{O}_2$ catalysts calcined at different temperatures

support. The enhancement of the catalytic activity of the ternary catalysts should be attributed to a synergistic effect between CuO and the binary supports. Meanwhile, the two $\text{CuO}/\text{Ti}_{0.8}\text{Ce}_{0.2}\text{O}_2$ and CuO/CeO_2 catalysts show much higher catalytic activity than the CuO/TiO_2 catalyst. The results are consistent with the XRD and TPR analyses. In contrast to the two $\text{CuO}/\text{Ti}_{0.8}\text{Ce}_{0.2}\text{O}_2$ and CuO/CeO_2 catalysts, in the XRD pattern of CuO/TiO_2 , the CuO diffraction peaks can be observed clearly, indicating larger particle size of bulk CuO, which less contributes to enhanced catalytic activity. Meanwhile, due to the addition of CeO_2 into TiO_2 inhibiting the transition phase from anatase to rutile, the $\text{CuO}/\text{Ti}_{0.8}\text{Ce}_{0.2}\text{O}_2$ sample exhibits very broad peaks with only a little of TiO_2 anatase phase, indicating the high dispersion of the small particle size CuO nanoparticles on the surface of the support, which should be responsible for the high catalytic activity of low-temperature CO oxidation. From the H_2 -TPR analysis, the TPR profile of CuO/TiO_2 shows no α peaks due to the reduction of highly dispersed CuO interacting strongly with the support, while the appearance of strong high temperature γ reduction peak indicates the existence of a large amount of bulk CuO which contributes little to the enhanced catalytic activity. Therefore, the absence of the highly dispersed small particle size CuO and presence of a large amount of bulk CuO with large particle size should be responsible for the lower activity of CuO/TiO_2 . Similarly, the existence of highly dispersed CuO in the two CuO/CeO_2 and $\text{CuO}/\text{Ti}_{0.8}\text{Ce}_{0.2}\text{O}_2$ catalysts contributes to their high catalytic activity. However, one can easily find that the α peak in $\text{CuO}/\text{Ti}_{0.8}\text{Ce}_{0.2}\text{O}_2$ catalyst is evidently stronger than in the CuO/CeO_2 catalyst, indicating more highly dispersed CuO in the $\text{CuO}/\text{Ti}_{0.8}\text{Ce}_{0.2}\text{O}_2$ catalyst, which results in higher activity of $\text{CuO}/\text{Ti}_{0.8}\text{Ce}_{0.2}\text{O}_2$ catalyst than the CuO/CeO_2 catalyst.

In order to investigate the catalyst stability, we studied the variation of the catalytic activity with the reaction time. Fig. 8 shows the conversion of CO over the $\text{CuO}/\text{Ti}_{0.8}\text{Ce}_{0.2}\text{O}_2$ catalyst calcined at 500 °C versus reaction time at the reaction temperature of 125 °C. It can be found that the catalyst shows no change in catalytic

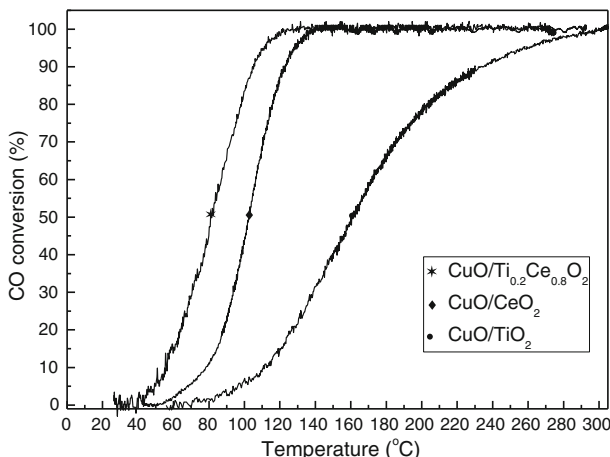


Fig. 7 Catalytic activity for CO oxidation of CuO/TiO₂, CuO/CeO₂ and CuO/Ti_{0.8}Ce_{0.2}O₂ calcined at 500 °C

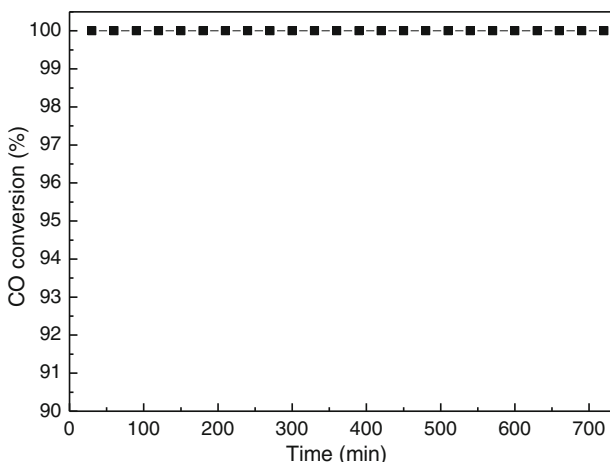


Fig. 8 Conversion of CO over the CuO/Ti_{0.8}Ce_{0.2}O₂ catalyst calcined at 500 °C versus reaction time

activity and maintains 100% conversion of CO during the period of reaction of 720 min. This demonstrates that the good catalytic stability is obtained for the as-prepared CuO/Ti_{0.8}Ce_{0.2}O₂ catalyst.

Conclusions

Ternary nanostructured CuO/Ti_{0.8}Ce_{0.2}O₂ catalysts with high-surface areas have been prepared by a one step surfactant-assisted method of nanoparticle assembly. The CuO/Ti_{0.8}Ce_{0.2}O₂ catalyst calcined at 500 °C with higher surface area and smaller particle size exhibits high catalytic activity and good stability on CO

oxidation with $T_{50\%}$ and $T_{100\%}$ at 82 and 123 °C. According to the XRD and BET analyses, the decrease in catalytic activity of the $\text{CuO}/\text{Ti}_{0.8}\text{Ce}_{0.2}\text{O}_2$ catalysts can be attributed to the decrease of the surface areas and the increase of particle sizes with the increase of calcination temperature. From the TGA result, the catalyst calcined at 400 °C with the largest surface area of 180 m²/g has lower activity than the catalyst calcined at 500 °C, which should be related to the existence of remained carbon species which was not completely removed after calcination of 400 °C. CuO supported on binary $\text{Ti}_{0.8}\text{Ce}_{0.2}\text{O}_2$ support show higher catalytic activity than CuO supported on single CeO_2 or TiO_2 support. In contrast to the two $\text{CuO}/\text{Ti}_{0.8}\text{Ce}_{0.2}\text{O}_2$ and CuO/CeO_2 catalysts, CuO/TiO_2 shows much lower catalytic activity. According to XRD and TPR analyses, absence of the highly dispersed small particle size CuO and existence of a large amount of bulk CuO with large particle size should be responsible for the lower activity of CuO/TiO_2 . Similarly, the existence of highly dispersed CuO in the two CuO/CeO_2 and $\text{CuO}/\text{Ti}_{0.8}\text{Ce}_{0.2}\text{O}_2$ catalysts contributes to their high catalytic activity. More highly dispersed CuO in the $\text{CuO}/\text{Ti}_{0.8}\text{Ce}_{0.2}\text{O}_2$ catalyst than in the CuO/CeO_2 catalyst results in more activity of $\text{CuO}/\text{Ti}_{0.8}\text{Ce}_{0.2}\text{O}_2$ catalyst than the CuO/CeO_2 catalyst.

Acknowledgment This work was supported by the National Natural Science Foundation of China (No. 20871071) and the Applied Basic Research Programs of Science and Technology Commission Foundation of Tianjin (Nos. 09JCYBJC03600 and 10JCYBJC03900).

References

1. Xu HY, Chu W, Luo JJ, Liu M (2010) New $\text{Au}/\text{FeOx}/\text{SiO}_2$ catalysts using deposition–precipitation for low-temperature carbon monoxide oxidation. *Catal Comm* 11:812–815
2. Seo PW, Choi HJ, Hong SI, Hong SC (2010) A study on the characteristics of CO oxidation at room temperature by metallic Pt. *J Hazard Mater* 178:917–925
3. Kunkalekar RK, Salker AV (2010) Low temperature carbon monoxide oxidation over nanosized silver doped manganese dioxide catalysts. *Catal Comm* 12:193–196
4. Mariño F, Descorme C, Duprez D (2005) Supported base metal catalysts for the preferential oxidation of carbon monoxide in the presence of excess hydrogen (PROX). *Appl Catal B* 58:175–183
5. Huang J, Wang SR, Zhao YQ, Wang XY, Wang SP, Wu SH, Zhang SM, Huang WP (2006) Synthesis and characterization of CuO/TiO_2 catalysts for low-temperature CO oxidation. *Catal Comm* 7:1029–1034
6. Cheng T, Fang Z, Hu Q, Han K, Yang X, Zhang Y (2007) Low-temperature CO oxidation over $\text{CuO}/\text{Fe}_2\text{O}_3$ catalysts. *Catal Comm* 8:1167–1171
7. Astudillo J, Águila G, Díaz F, Guerrero S, Araya P (2010) Study of $\text{CuO}–\text{CeO}_2$ catalysts supported on SiO_2 on the low-temperature oxidation of CO. *Appl Catal A* 381:169–176
8. Ma XD, Sun HW, Sun Q, Feng X, Guo HW, Fan B, Zhao S, He X, Lv L (2011) Catalytic oxidation of CO and *o*-DCB over CuO/CeO_2 catalysts supported on hierarchically porous silica. *Catal Comm* 12:426–430
9. Shiau CY, Ma MW, Chuang CS (2006) CO oxidation over CeO_2 -promoted $\text{Cu}/\gamma\text{-Al}_2\text{O}_3$ catalyst: effect of preparation method. *Appl Catal A* 301:89–95
10. Zheng XC, Wu SH, Wang SP, Wang SR, Zhang SM, Huang WP (2005) The preparation and catalytic behavior of copper-cerium oxide catalysts for low-temperature carbon monoxide oxidation. *Appl Catal A* 283:217–223
11. Zhu H (2004) $\text{Pd}/\text{CeO}_2/\text{TiO}_2$ catalyst for CO oxidation at low temperature: a TPR study with H_2 and CO as reducing agents. *J Catal* 225:267–277
12. Lamalle M, Ayadi HE, Gennequin C, Cousin R, Siffert S, Aïssi F, Aboukaïs A (2008) Effect of the preparation method on $\text{Au}/\text{Ce-Ti-O}$ catalysts activity for VOCs oxidation. *Catal Today* 137:367–372

13. Gennequin C, Lamalle M, Cousin R, Siffert S, Aïssi F, Aboukaïs A (2007) Catalytic oxidation of VOCs on Au/Ce-Ti-O. *Catal Today* 122:301–306
14. Zou ZQ, Meng M, Guo LH, Zha YQ (2009) Synthesis and characterization of CuO/Ce_{1-x}Ti_xO₂ catalysts used for low-temperature CO oxidation. *J Hazard Mater* 163:835–842
15. Zhou RX, Yu TM, Jiang XY, Chen F, Zheng XM (1999) Temperature-programmed reduction and temperature-programmed desorption studies of CuO/ZrO₂ catalysts. *Appl Surf Sci* 148:263–270
16. Lin R, Luo MF, Zhong YJ, Yan ZL, Liu GY, Liu WP (2003) Comparative study of CuO/Ce_{0.7}Sn_{0.3}O₂, CuO/CeO₂ and CuO/SnO₂ catalysts for low-temperature CO oxidation. *Appl Catal A* 255:331–336
17. Liu Z, Zhou R, Zheng X (2008) Preferential oxidation of CO in excess hydrogen over a nanostructured CuO-CeO₂ catalyst with high surface areas. *Catal Comm* 9:2183–2186
18. Tang X, Zhang B, Li Y, Xu Y, Xin Q, Shen W (2005) CuO/CeO₂ catalysts: redox features and catalytic behaviors. *Appl Catal A* 288:116–125
19. Yao HC, Yao YFY (1984) Ceria in automotive exhaust catalysts: I oxygen storage. *J Catal* 86: 254–265
20. Jiang XY, Ding GH, Lou LP, Chen YX, Zheng XM (2004) Catalytic activities of CuO/TiO₂ and CuO-ZrO₂/TiO₂ in NO + CO reaction. *J Mol Catal A* 218:187–195
21. Zheng XC, Wang SP, Wang SR, Zhang SM, Huang WP, Wu SH (2005) Preparation, characterization and catalytic properties of CuO/CeO₂ system. *Mater Sci Eng C* 25:516–520
22. Wang SP, Zhang TY, Wang XY, Zhang SM, Wang SR, Huang WP, Wu SH (2007) Synthesis, characterization and catalytic activity of Au/Ce_{0.8}Zr_{0.2}O₂ catalysts for CO oxidation. *J Mol Catal A* 272:45–52
23. Nelson AE, Schulz KH (2003) Surface chemistry and microstructural analysis of Ce_xZr_{1-x}O_{2-y} model catalyst surfaces. *Appl Surf Sci* 210:206–221
24. Zhang YW, Si R, Liao CS, Yan CH, Xiao CX, Kou Y (2003) Facile alcothermal synthesis, size-dependent ultraviolet absorption and enhanced CO conversion activity of ceria nanocrystals. *J Phy Chem B* 107:10159–10167
25. Larsson PO, Andersson A (1998) Complete oxidation of CO ethanol, and ethyl acetate over copper oxide supported on titania and ceria modified titania. *J Catal* 179:72–89
26. Avgoustopoulos G, Ioannides T (2003) Selective CO oxidation over CuO-CeO₂ catalysts prepared via the urea-nitrate combustion method. *Appl Catal A* 244:155–167
27. Wang SP, Zheng XC, Wang XY, Wang SR, Zhang SM, Yu LH, Huang WP, Wu SH (2005) Comparison of CuO/Ce_{0.8}Zr_{0.2}O₂ and CuO/CeO₂ catalysts for low-temperature CO oxidation. *Catal Lett* 105:163–168
28. Kundakovic L, Flytzani-Stephanopoulos M (1998) Reduction characteristics of copper oxide in cerium and zirconium oxide systems. *Appl Catal A* 171:13–29
29. Zhu HY, Shen MM, Kong Y, Hong JM, Hu YH, Liu TD, Dong L, Chen Y, Jian C, Liu Z (2004) Characterization of copper oxide supported on ceria-modified anatase. *J Mol Catal A* 219:155–164
30. Busca G, Costantino U, Marmottini F, Montanari T, Patrono P, Pinzari F, Ramis G (2006) Methanol steam reforming over ex-hydrotalcite Cu-Zn-Al catalysts. *Appl Catal A* 310:70–78